International Journal of Innovative
Computing, Information and Control
Volume **15**, Number **4**, August **2019**

ICIC International ©2019 ISSN 1349-4198
pp. **1309–1322**

FACE RECOGNITION USING SHEARLETS EDGES FUSION

Huixian Yang, Weifa Gan, Fan Chen and Xiaoxiao Li

College of Physics and Optoelectronic Engineering
Xiangtan University
Yanggutang, Yuhu District, Xiangtan 411105, P. R. China
hxyangxt@gmail.com

Received November 2018; revised March 2019

Abstract. *In this paper, to save significant edges, we propose an algorithm of face recognition using shearlets edges fusion (Shearlets_EF). Firstly, the original images are decomposed into subimages by applying the shearlet transform. Then the directional subimages are fused by the maximum modulus principle. Thirdly, dividing fused images into patches, facial features of each patch are extracted by using uniform local binary pattern (ULBP) only with 2 times variations (ULBPO2V). Finally, face images are classified by collaborative representation based classification (CRC). Testing in the databases of AR, CMUPIE, Extended Yale B, and LFW, experimental results illustrate that Shearlets_EF has better performance compared to relative algorithms.*
Keywords: Face recognition, The shearlet transform, Edges feature, Uniform local binary pattern

1. **Introduction.** Face recognition has received significant attention due to its potential value for applications. Up to now, many approaches have been introduced to deal with face recognition, such as wavelet transform [1-3], support vector machine [4-6], and artificial neural network [7-9].

Shearlet transform, a new multiscale method introduced by Guo et al. [13,14], has emerged in recent years, which goes beyond traditional wavelets for the ability to capture anisotropic information. One particularly appealing feature of shearlets is that it combines a multiscale framework which is particularly effective to capture the facial geometry, together with a simple mathematical construction which can be associated to a multiresolution analysis and enables fast numerical processing [15].

Some researchers tackle face recognition problems by using the shearlets [16-18]. Borgi et al. [15] proposed a face recognition method that combines shearlet networks (SN) and PCA called SNPCA. SNPCA uses the power of multiscale representation with a unique ability to capture geometric information to derive a very efficient representation of facial templates. Huang et al. [19] proposed a difference shearlet characteristic of fast sparse description method to address face recognition problem, using a matching score fusion strategy to fuse the amplitude and phase coding of shearlet features at different scales. Schwartz et al. [20] developed a feature descriptor, the histograms of shearlet coefficients (HSC), based on the shearlet transform for its accurate multiscale analysis. HSC is obtained by the concatenation of the histograms estimated for each decomposition level. Zhang et al. [21] proposed a method for face recognition based on shearlet multi-orientation adaptive weighted fusion and sparse representation. By using the energy and mean characteristics of directional subimages in each level, the human face subimages are weighed and fused.

DOI: 10.24507/ijicic.15.04.1309

The original image will be decomposed into subimages with multiscale and multidirection by using the shearlet transform. To decrease dimensions, some algorithms accumulate subimages in each scale and then average them, named average fusion in this paper. For example, Shearlet_ULBP [22] fuses averagely all directional subimages of each level obtained by using the shearlets. HLSPQ [23] uses the average fusion method to fuse the original shearlet features of the same scale. However, using the algorithm of average fusion, some facial details will be weakened and the contrast of the fused image will be reduced, resulting in fuzzing facial edges to some extent. Thus, it is not equally well, using the average fusion method, to preserve the significant facial edges which play an important role in face recognition because it contains rich information related to facial organ and texture classification. On the other hand, Shearlet_ULBP divides the fused images into plenty of patches and extracts the features of each patch by exploiting the histogram of the uniform local binary pattern (ULBP), whereas, the dimension of integrated features is relatively large. Based on the discussion above, we propose an algorithm of face recognition using shearlets edges fusion (Shearlets_EF).

The main contribution of this paper can be summarized as follows. Firstly, we figure out a principle of the maximum modulus to fuse directional subimages obtained by using the shearlets, which saves significant edges and preserves the structural attributes of the face image. Secondly, to reduce histogram dimensions, we exploit uniform local binary pattern (ULBP) only with 2 times variations (ULBPO2V) to extract patches features, which reduces the dimension of the histogram to 57 from 59. We also note that ULBPO2V performs better than ULBP when patches number is 9×9. Thirdly, we investigate the effect of the number of decomposed orientations of the shearlets and divided patches of the fused image on face recognition.

The rest of this paper is organized as follows. Section 2 describes the related works. Section 3 introduces the Shearlets_EF in detail. Section 4 conducts experiments and analysis. Conclusions are made in Section 5.

2. Related Works.

As mentioned above, the contribution of this paper mainly reflects in the proposed algorithm of fusing directional subimages obtained by using the shearlet transform and reducing the dimensions of the histogram to 57 from 59 by using ULBPO2V originated from ULBP. To better illustrate the Shearlets_EF, we first introduce the shearlet transform and original ULBP, as well as CRC classifier in this section.

2.1. The shearlet transform.

The shearlet transform is a genuinely multidimensional version of the conventional wavelet transform and is especially designed to represent data containing anisotropic and directional feature with high efficiency. Thus, this approach provides optimally sparse approximations for images with edges, outperforming traditional wavelets. Shearlets decomposition for two levels is illustrated in Figure 1. Formally, the continuous shearlet transform [24] for signal ξ is defined as the mapping:

$$SH_\psi(a,s,t) = \langle \xi, \psi_{a,s,t} \rangle, \quad a > 0,\ s \in \mathbb{R},\ t \in \mathbb{R}^2 \tag{1}$$

where the analyzing factor $\psi_{a,s,t}$ is called shearlet basis, defined as

$$\psi_{a,s,t}(x) = |\det M_{as}|^{-\frac{1}{2}} \psi\left(M_{as}^{-1}(x-t)\right),$$

and $M_{as} = \begin{bmatrix} a & s\sqrt{a} \\ 0 & \sqrt{a} \end{bmatrix}$, each matrix M_{as} can be factorized as $B_s A_a$, where $B_s = \begin{bmatrix} 1 & s \\ 0 & 1 \end{bmatrix}$ is a shear matrix, and $A_a = \begin{bmatrix} a & 0 \\ 0 & \sqrt{a} \end{bmatrix}$ is an anisotropic dilation matrix.

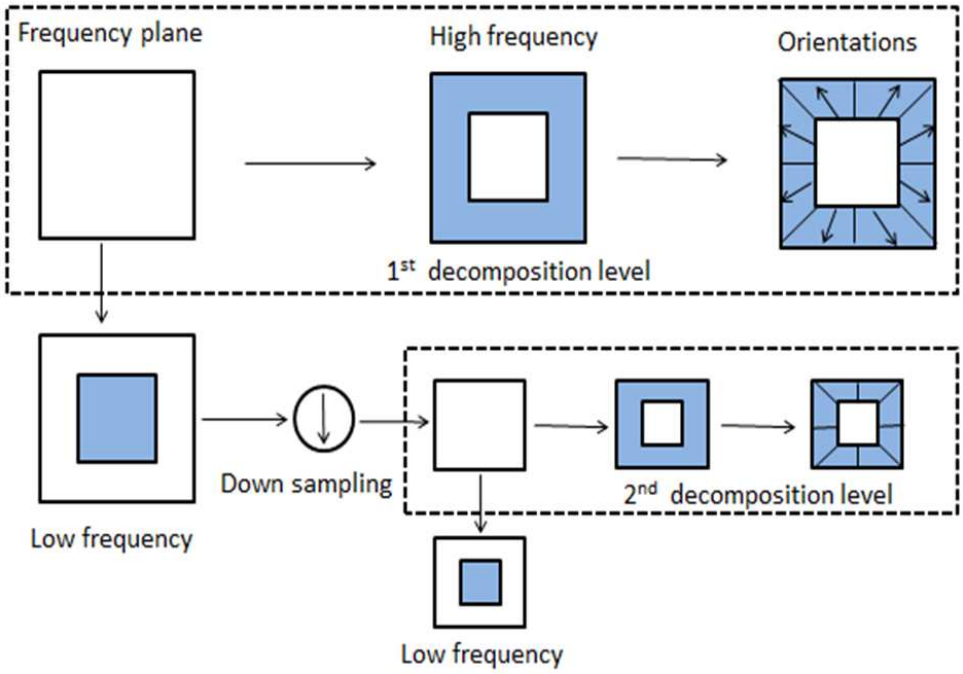

FIGURE 1. Shearlets decomposition for two levels

2.2. **Uniform local binary pattern.** The original local binary pattern (LBP) operator was proposed by Ojala et al. [25]. The neighborhood pixels, by taking the gray value of the center pixel as a threshold, are converted to binary code 0 or 1, and then all these codes form an ordered pattern (end to end), as shown in Figure 2. Usually, we choose 8 sampling points; thus, there are 256 dimensions in the original LBP histogram. To lessen the dimensions, LBP of uniform pattern (ULBP), which the variations of its ordered patterns, i.e., 0 to 1 and 1 to 0, are at most 2 times, was presented by Ojala et al. The dimensions of ULBP histogram are decreased to 59 in that there are 58 kinds of uniform pattern and others are regarded as one class.

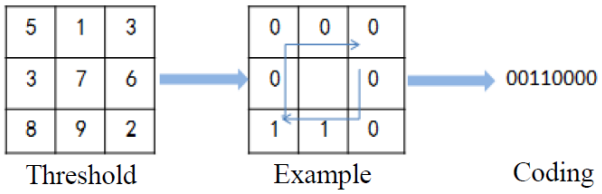

FIGURE 2. An example of basic LBP operator

2.3. **Collaborative representation based classification.** Zhang et al. [26] proposed a collaborative representation based classification (CRC) of face images by using the regularized least square model. Denote by $\boldsymbol{X}_k \in \mathbb{R}^{m\times n}$, the set of gallery samples from class k. Suppose that we have the c class of subjects and let $\boldsymbol{X} = [\boldsymbol{X}_1, \boldsymbol{X}_2, \boldsymbol{X}_k, \ldots, \boldsymbol{X}_c]$. Given a query sample $\boldsymbol{y}$, CRC codes $\boldsymbol{y}$ over $\boldsymbol{X}$ by

$$\boldsymbol{a}' = \arg\min_{\boldsymbol{a}} \left\{ \|\boldsymbol{y} - \boldsymbol{X}\boldsymbol{a}\|_2^2 + \lambda \|\boldsymbol{a}\|_2^2 \right\} \tag{2}$$

where $\boldsymbol{a}$ and λ are coefficient vector and regularization parameter respectively. Equation (2) can be solved by $\boldsymbol{a}' = \left(\boldsymbol{X}^T\boldsymbol{X} + \lambda \boldsymbol{I}\right)^{-1} \boldsymbol{X}^T\boldsymbol{y}$. Then the error can be computed by $\boldsymbol{r}_k = \|\boldsymbol{y} - \boldsymbol{X}_k\boldsymbol{a}'_k\|/\|\boldsymbol{a}'_k\|_2$. At last, $\boldsymbol{y}$ is classified by $\mathit{Identity}(\boldsymbol{y}) = \arg\min_k\{\boldsymbol{r}_k\}$. The process of CRC is summarized in Table 1.

TABLE 1. The algorithm of CRC

CRC codes $\boldsymbol{y}$ over $\boldsymbol{X}$
$$\boldsymbol{a}' = \arg\min_{\boldsymbol{a}} \{\|\boldsymbol{y} - \boldsymbol{X}\boldsymbol{a}\|_2^2 + \lambda\|\boldsymbol{a}\|_2^2\} \quad (3)$$
Computing the solution of Equation (2)
$$\boldsymbol{a}' = \left(\boldsymbol{X}^T\boldsymbol{X} + \lambda\boldsymbol{I}\right)^{-1}\boldsymbol{X}^T\boldsymbol{y} \quad (4)$$
Next step, the error is computed by
$$\boldsymbol{r}_k = \|\boldsymbol{y} - \boldsymbol{X}_k\boldsymbol{a}'_k\|/\|\boldsymbol{a}'_k\|_2 \quad (5)$$
$\boldsymbol{y}$ is classified by
$$Identity(\boldsymbol{y}) = \arg\min_k\{\boldsymbol{r}_k\} \quad (6)$$

3. Face Recognition Using Shearlets Edges Fusion.

3.1. **General framework for Shearlets_EF.** In this section, we describe the general framework for Shearlets_EF. Figure 3 shows the procedure of Shearlets_EF. First of all, the face images are decomposed into subimages with multiscale and multidirection by applying the shearlet transform. We assume that scale $j = 0, 1, 2, \ldots, L$, where $j = 0$ corresponds to the low frequency and $j = 1, 2, \ldots, L$ corresponds to the coarse to fine scales. In the scale $j = 0$, there is only one subimage with low frequency, while there are multidirectional subimages in each scale $j = 1, 2, \ldots, L$. Then the multidirectional subimages in the same scale ($j = 1, 2, \ldots, L$) are fused into one image by using the maximum modulus principle (please note that, in this step, the subimage with the low frequency is not processed, but it is waiting to be treated in the next step). At that time, $L - 1$ fused images are yielded.

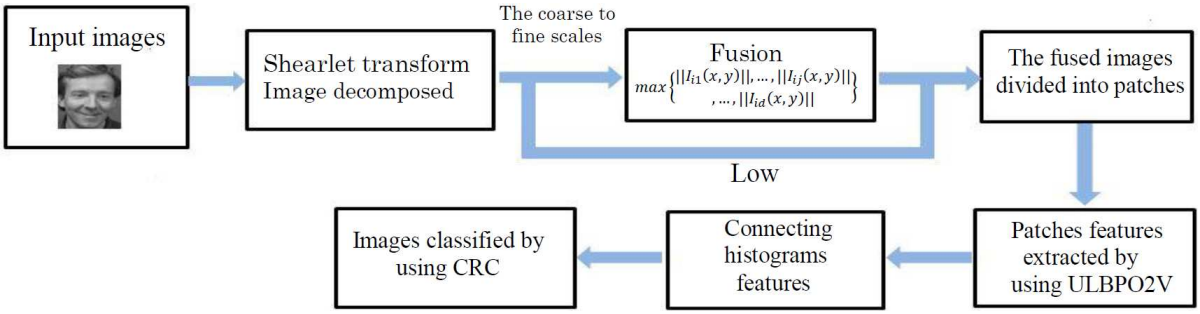

FIGURE 3. The procedure of Shearlets_EF

At last, dividing the $L - 1$ fused images and the subimage with low frequency (L images processed totally) into $n \times n$ patches respectively, facial features of each patch are extracted by using ULBPO2V, which generates $L \times n \times n$ ULBPO2V histograms features. And then the patches features of the ULBPO2V histograms from the same image are connected into one histogram feature, producing L histograms features totally. In the process of image classification, the L histograms features are reshaped into one vector to feed CRC classifier.

For the coarse to fine scales, taking 3 scales and 10 directions decomposition for instance, directional subimages at different levels are shown in Figure 4. Figure 5 illustrates the general framework for extracting features.

3.2. **Image fusion using the maximum modulus principle.** When fusing subimages, we exploit the maximum modulus principle, instead of the average fusion. For the coarse to fine scales, the relatively max moduli are corresponding to significant features such as

(a) Original image

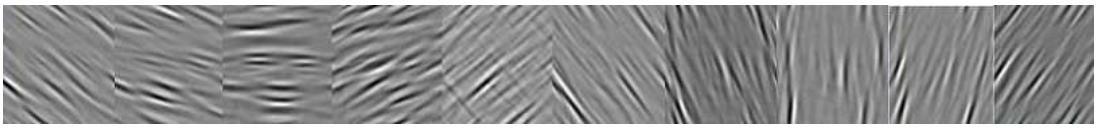

(b) Decomposed subimages in the 1st level

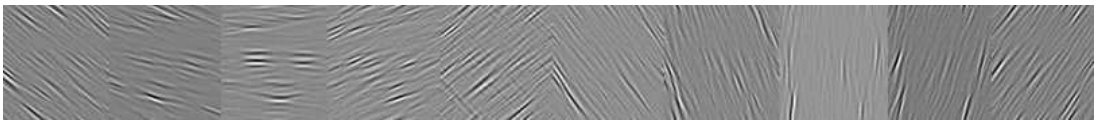

(c) Decomposed subimages in the 2nd level

(d) Decomposed subimages in the 3rd level

FIGURE 4. Decomposed subimages of the shearlet transform (The 1st to the 10th directional subimages from left to right in order)

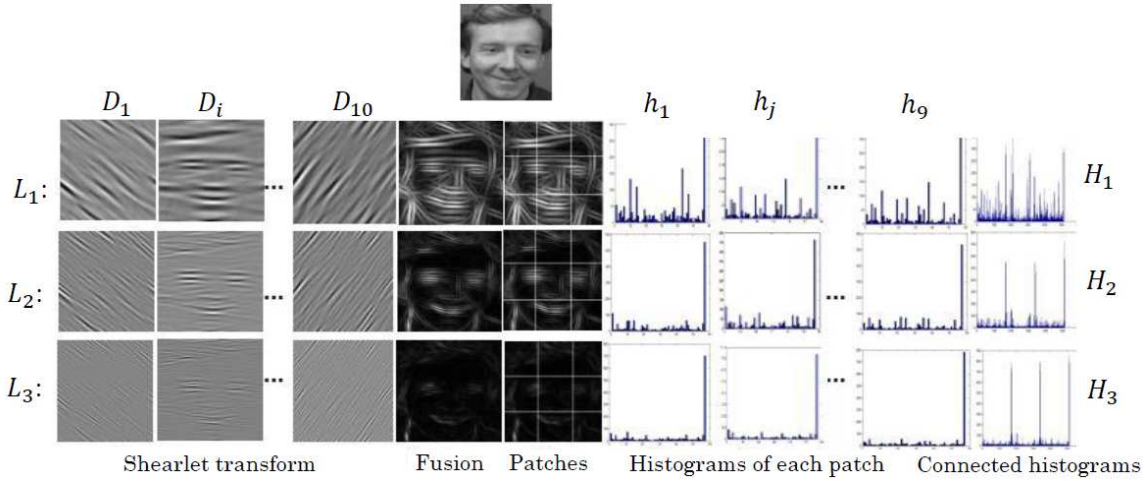

FIGURE 5. General framework for extracting feature. L_1 to L_3 represent the subimages of the shearlets from the 1st level to the 3rd level, respectively. D_i means the subimages of the shearlets in the i^{th} direction. h_j describes the histogram features of the j^{th} patch. H_1 to H_3 represent the features of the fused images from the 1st level to the 3rd level, respectively. The connected histogram is formed by $[h_1, h_2, \ldots, h_9]$ in each level.

the edges. Subimages of these scales are fused by using Equation (7), which can save significant edges features.

$$I'_i(x,y) = \max\{\|I_{i1}(x,y)\|, \ldots, \|I_{ij}(x,y)\|, \ldots, \|I_{id}(x,y)\|\},\ 1 < j < d,\ i = 1, 2, \ldots, L \quad (7)$$

where i and j, respectively, represent the i^{th} level and the j^{th} direction of the shearlet transform. L and d stand for the total number of levels and directions in the i^{th} level respectively. $I_{ij}(x,y)$ represents the pixel value in the position (x,y) of the subimage of the j^{th} direction in the i^{th} level and $I'_i(x,y)$ represents pixel value in the position (x,y) of the fused image in the i^{th} level. Namely, we compute the moduli of pixel values for all subimages in each level and then we choose the maximum modulus as the fused pixel in the corresponding position.

Figure 6 shows an example and the values in the red circle are in the position $(1,3)$ for each directional subimage. Firstly, we compute moduli for all pixel values. Secondly, if we want to obtain the fused pixel value in the position $(1,3)$, we need to compare pixel values in that position of all directional subimages. Namely, the pixel values in the red circle from the 1st directional subimage to the 4th directional subimage will be compared. From Figure 6, we can know that there are 0.3231, 0.2236, 0.2022, 0.2022 in the position $(1,3)$ of all directional subimages. We choose 0.3231, the maximum modulus compared to 0.2236, 0.2022, 0.2022 these moduli, to be the fused pixel in the position $(1,3)$. We also obtain fused pixel values in other positions and the like, generating a fused image.

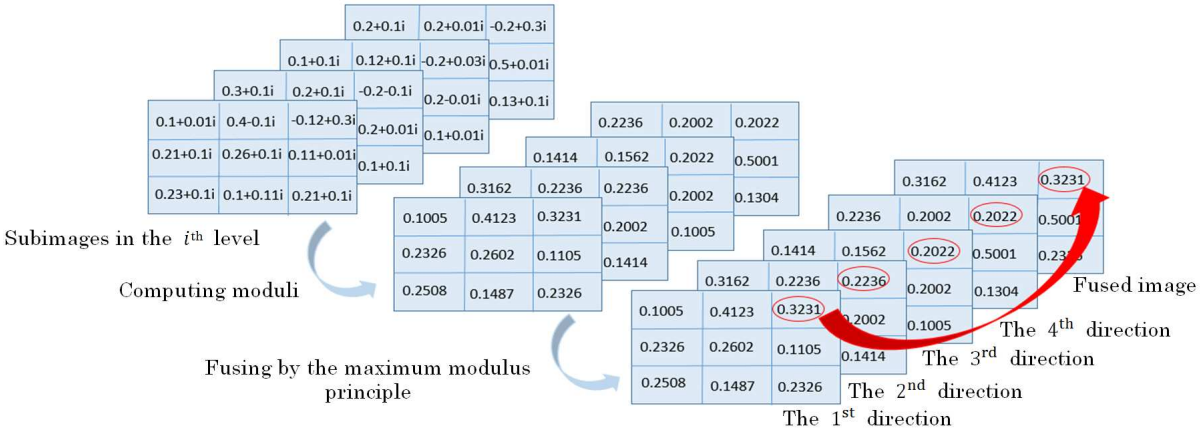

FIGURE 6. An example of fusion by the maximum modulus principle

Images fused by the maximum modulus principle and the average fusion are compared in Figure 7. According to Figure 7, we can see that Figure 7(a) retains more significant edges, illustrating that the maximum modulus fusion outstrips the average fusion in the aspect of holding the significant edges.

3.3. **Dividing images into patches and extracting features using ULBPO2V.** Histogram describes image features as a whole, whereas, a lot of structural details will be ignored when it describes the face image directly. To obtain more local features, we divide the image into patches and describe the features of each patch by the histogram of ULBPO2V.

As mentioned in Section 2.2, the dimensions of ULBP histogram are 59 in that there are 58 classes of uniform pattern and other patterns (non-uniform pattern) are regarded as one class. The variations of 1 to 0 and 0 to 1 of uniform pattern are at most 2 times, i.e., 0 time or 2 times (without 1 time). Among 58 classes of uniform pattern, there are 2 classes of uniform patterns with 0 time variation, i.e., 00000000 and 11111111 and 56

(a) (b)

FIGURE 7. Comparing fused images (The image in Figure 7(a) is fused by the maximum modulus principle while the image in Figure 7(b) is fused by the average fusion method)

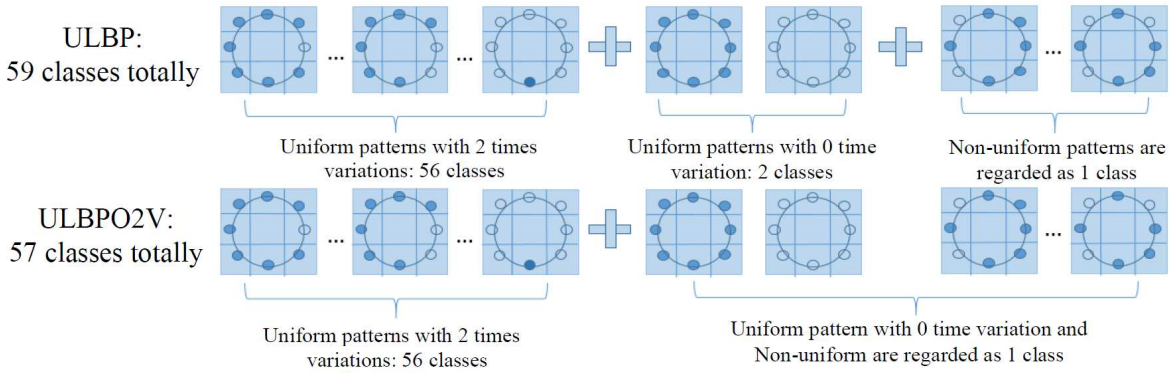

FIGURE 8. The difference between ULBP and ULBPO2V (Filled circles and unfilled circles stand for 1 and 0 respectively)

classes of uniform patterns with 2 times variations, such as 10000000, 11000000 and so on. Original ULBP has 59 classes totally. Original ULBP will compute the number of each class; thus, if we use the original ULBP to describe the features, we will obtain $[\alpha_1, \alpha_2, \ldots, \alpha_i, \ldots, \alpha_{59}]$, where α_i stands for the number of the i^{th} class of ULBP. In this paper, given that the number of the uniform patterns with 0 time variation is small; thus, we regard the uniform patterns with 0 time variation and the non-uniform patterns as one class. As shown in Figure 8, the dimensions of ULBPO2V are reduced to $56+1$ from $56+2+1$; thus, if we use the original ULBP to describe the features, we will obtain $[\beta_1, \beta_2, \ldots, \beta_j, \ldots, \beta_{57}]$, where β_j represents the number of the j^{th} class of ULBPO2V. For each histogram, we can reduce 2 dimensions if we use the proposed ULBPO2V, instead of the original ULBP, to extract features.

Taking the shearlet transform with 4 levels decomposition for example, there are four images including three fused images of the coarse to fine scales and one image with the low frequency. In these four images, if each image is divided into 10×10 patches, then we have 400 patches totally and decrease 400×2 dimensions. Table 2 shows the relationship between patches number and decreased dimensions.

4. **Experimental Results and Analysis.** In this section, to test the performance of Shearlets_EF, we conduct experiments 20 times in the databases of AR [27], CMUPIE [28], Extended Yale B [29], and LFW [30] respectively, which have been widely used to evaluate

TABLE 2. Relationship between patches number and decreased dimensions

Patches number	Decreased dimensions
3×3	72
4×4	128
5×5	200
6×6	288
7×7	392
8×8	512
9×9	648
10×10	800

algorithms of face recognition. We compare Shearlets_EF with classical algorithms PCRC [33], CRC [26] and recent algorithms RSLDA [31], SPN-DL [32], Shearlet_ULBP [22].

The input images are set to 128×128 pixels and the sizes of directional filters are set to 60×60. The numbers of decomposed levels and directions are set to 3 and 10 respectively. The number of patches is fixed to 9×9. In the CRC, normalized parameter λ is set to 0.005 as [22].

4.1. **Testing for face recognition rate.** AR includes 3120 different images from 120 individuals, which were taken under five different conditions containing normal, expression, illumination, 20% occlusion, and 40% occlusion. Two images were taken in the normal condition for each individual and six images in every abnormal condition. The gallery set of each class is produced by two normal images and the rest of the images of each class are made up the probe set.

Table 3 reports the experimental data. The face variations in the uncontrolled environment lead to poor accuracy for most methods. Nonetheless, Shearlets_EF still works well relatively. For one thing, we can see that both Shearlets_EF and Shearlet_ULBP perform better than RSLDA, SPN-DL, PCRC, and CRC in these different conditions. For another, from 20% occlusion to 40% occlusion, the accuracies of RSLDA, SPN-DL, PCRC and CRC drop 60.27%, 38.34%, 20.98% and 34.03% respectively, while Shearlet_ULBP, and Shearlets_EF only drop 10.14% and 8.06% respectively. It indicates that the shearlets also have strong ability to extract effective features, especially the ability to capture anisotropic information, even though in the condition of illumination, expression and occlusion. Shearlets_EF outstrips Shearlet_ULBP, especially in the condition of 40% occlusion, which demonstrates that the maximum modulus fusion holds greater advantages than the average fusion. Even though under the condition of 40% occlusion, the accuracy of Shearlets_EF still achieves above 90%; thus, we can come to the conclusion that Shearlets_EF is not only relatively robust to illumination and expression, but also occlusion.

TABLE 3. Accuracies (%) tested in the AR

Methods	Illumination	Expression	20% occlusion	40% occlusion
RSLDA	75.69	92.08	92.08	31.81
SPN-DL	92.90	92.64	85.42	47.08
PCRC	89.58	80.69	77.79	56.81
CRC	95.28	94.44	86.67	52.64
Shearlet_ULBP	99.72	98.89	98.89	88.75
Shearlets_EF	**99.86**	**99.58**	**99.17**	**91.11**

The CMUPIE contains 68 subjects with 41368 face images as a whole. Images of each person were taken across 13 different poses, under 43 different illumination conditions, and with 4 different expressions. We choose a subset of images from the five near frontal poses of each person. There are 170 images per subject with all kinds of illuminations and expressions. 20 images and 60 images of each person are, respectively, selected randomly to be the gallery set and the probe set.

From Table 4, we can observe that, as the results in AR database, the accuracies of Shearlet_ULBP and Shearlets_EF are much higher than RSLDA, SPN-DL, PCRC and CRC, which also argues that the shearlets have outstanding ability to extract effective features. Though CMUPIE dataset contains 13 different poses, we can infer that, from the result, Shearlets_EF is not very sensitive to poses variation. In summary, our algorithm Shearlets_EF performs better than relative algorithms in this dataset.

TABLE 4. Accuracies (%) tested in the CMUPIE

Methods	Accuracies
RSLDA	68.62 ± 2.81
SPN-DL	69.41 ± 2.52
PCRC	69.07 ± 3.04
CRC	91.64 ± 1.67
Shearlet_ULBP	98.21 ± 0.79
Shearlets_EF	$\mathbf{98.43 \pm 0.69}$

Extended Yale B contains 2432 frontal images of 38 individuals, which were taken under varying illumination condition. 20 images and 44 images of each person are, respectively, selected randomly to be the gallery set and the probe set. Table 5 displays the results.

TABLE 5. Accuracies (%) tested in the Extended Yale B

Methods	Accuracies
RSLDA	87.86 ± 4.22
SPN-DL	64.27 ± 5.00
PCRC	99.51 ± 0.06
CRC	98.12 ± 1.22
Shearlet_ULBP	99.89 ± 0.09
Shearlets_EF	$\mathbf{99.91 \pm 0.09}$

From Table 5, we can see that PCRC, CRC, Shearlet_ULBP, and Shearlets_EF achieve relatively satisfactory results. The commonality of these four algorithms using the CRC classifier is part of the reason that they have higher accuracies. Though these four algorithms use the same classifier, Shearlets_EF achieves the best in that Shearlets_EF has the advantage of capturing features. In last database CMUPIE, CRC substantially exceeds PCRC while PCRC has higher accuracy compared to CRC in this database, which illustrates that PCRC is not stable enough and easily affected by the dataset variables, i.e., the cropping way and environment variations of the dataset. Compared to PCRC, Shearlets_EF is more stable, leading the best result so far, even though both PCRC and Shearlets_EF divide images into patches and use CRC classifier. To sum up, Shearlets_EF has stronger discrimination than compared algorithms and its recognition rate achieves 99.91%.

The LFW database contains images of 5,749 different individuals in an unconstrained environment. LFW-a is a version of LFW after alignment using commercial face alignment

software. We gather the subjects including no less than 10 samples and then get a dataset with 158 subjects from LFW-a. The gallery set of each class is yielded by 4 images selected randomly and the rest of the images of each class are made up the probe set. The results are listed in Table 6.

TABLE 6. Accuracies (%) tested in the LFW

Methods	Accuracies
RSLDA	22.30 ± 1.36
SPN-DL	28.41 ± 1.52
PCRC	23.80 ± 1.55
CRC	42.22 ± 1.83
Shearlet_ULBP	60.00 ± 1.44
Shearlets_EF	$\mathbf{61.11 \pm 1.44}$

Please pay attention that LFW dataset is extremely challenging. It is usually non-frontal face with lots of intraclass variations for each subject; therefore, the performance of all the algorithms is relatively poor. From Table 6, we can be aware that the accuracies of Shearlets_EF and Shearlet_ULBP greatly exceed RSLDA, SPN-DL, PCRC and CRC, about 20% to 40%, which reflects the superiority of the shearlets to capture the facial geometry. In the case of Shearlets_EF and Shearlet_ULBP substantially leading recognition rate, Shearlets_EF still overtops Shearlet_ULBP by 1.11%. From the results, it is clear that Shearlets_EF still holds advantages over compared methods even in the relatively big-scale and complex database.

Based on the above four experiments, we can observe that, compared to relative algorithms in this paper, Shearlets_EF performs more outstanding. We can analyze the underlying cause from two aspects. Firstly, we use the maximum modulus principle to fuse directional subimages, holding the significant edges which belong to the high frequency features, less sensitive to illumination, expression, occlusion and pose. Secondly, we divide the fused images and the low frequency subimage into patches and extract patches features by using ULBPO2V, which can obtain more local information.

4.2. **Testing for time consumption.** Under the same experiment condition, we test the time consumption including the process of extracting features and recognition for all compared algorithms in CMUPIE and Extended Yale B dataset. Table 7 reports the results. From Table 7, we can observe that, with regret, Shearlets_EF cannot achieve the best in terms of time due to the shearlet transform taking up more time, but it performs better than the recent algorithms RSLDA and Shearlet_ULBP.

We also investigate the influence of patches number on time consumption and compared with Shearlet_ULBP, the most similar algorithm with Shearlets_EF, as shown in Figure

TABLE 7. Time consumption(s)

Methods	CMUPIE	Extended Yale B
RSLDA	3177.08	2283.62
SPN-DL	56.98	23.77
PCRC	388.53	74.50
CRC	464.54	105.67
Shearlet_ULBP	1300.53	483.99
Shearlets_EF	**1289.93**	**481.87**

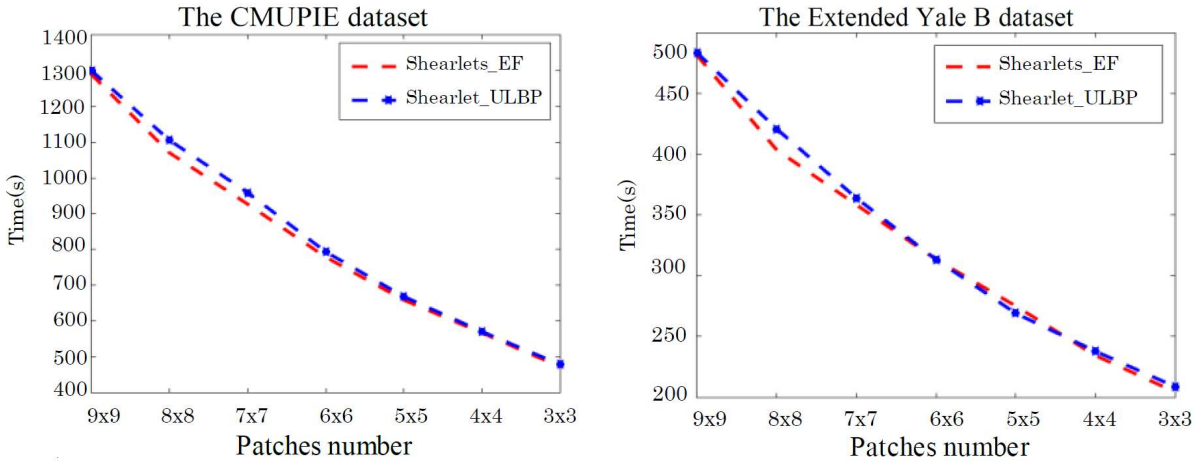

(a) In the CMUPIE dataset (b) In the Extended Yale B dataset

FIGURE 9. Time comparing with Shearlets_ULBP for different number

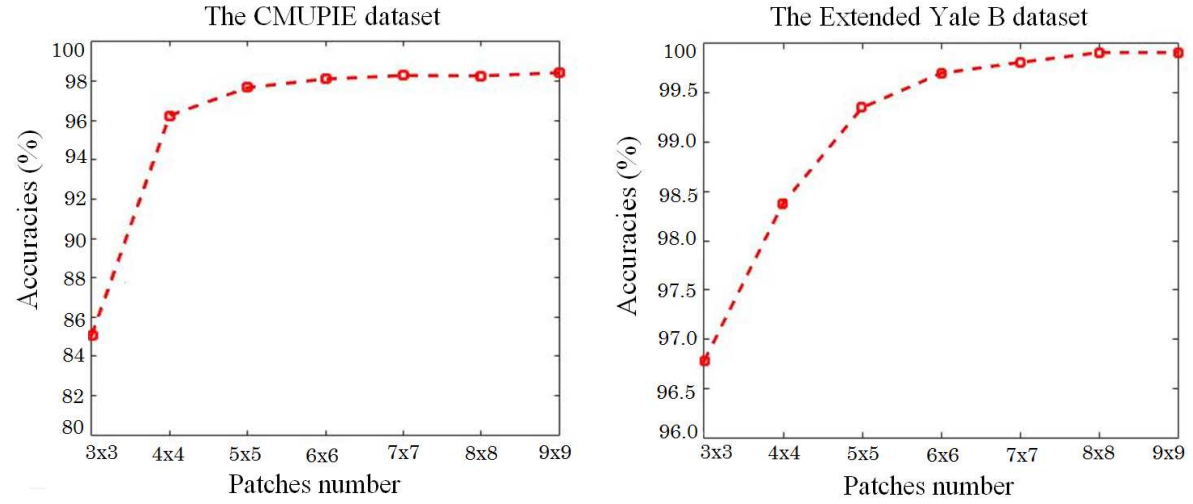

(a) In the CMUPIE dataset (b) In the Extended Yale B dataset

FIGURE 10. The effect of patches number

9. We can see that, from Figure 9, Shearlet_EF runs faster than Shearlet_ULBP almost in all different patches number.

4.3. **Investigating the effect of patches number.** For Shearlets_EF, patches number is an important influencing factor. We estimate the effect of patches number in CMUPIE, Extended Yale B database. Figure 10 shows the results. We can observe that Shearlets_EF is relatively sensitive to patches number. With the increasing of patches number, recognition rate grows fast and then grows gradually, because more local information can be obtained when patches number increases, but the function of the local information obtained tends to be saturated at a late period. When we set the patches number to 9×9, Shearlets_EF works relatively well.

4.4. **Comparing ULBPO2V and ULBP.** We compare ULBPO2V with ULBP in CMUPIE and Extended Yale B database. Figure 11 shows the results. We observe that ULBPO2V and ULBP do not make much difference but ULBPO2V performs little better in both datasets when the patches number is 9×9. Thus, we can make a conclusion

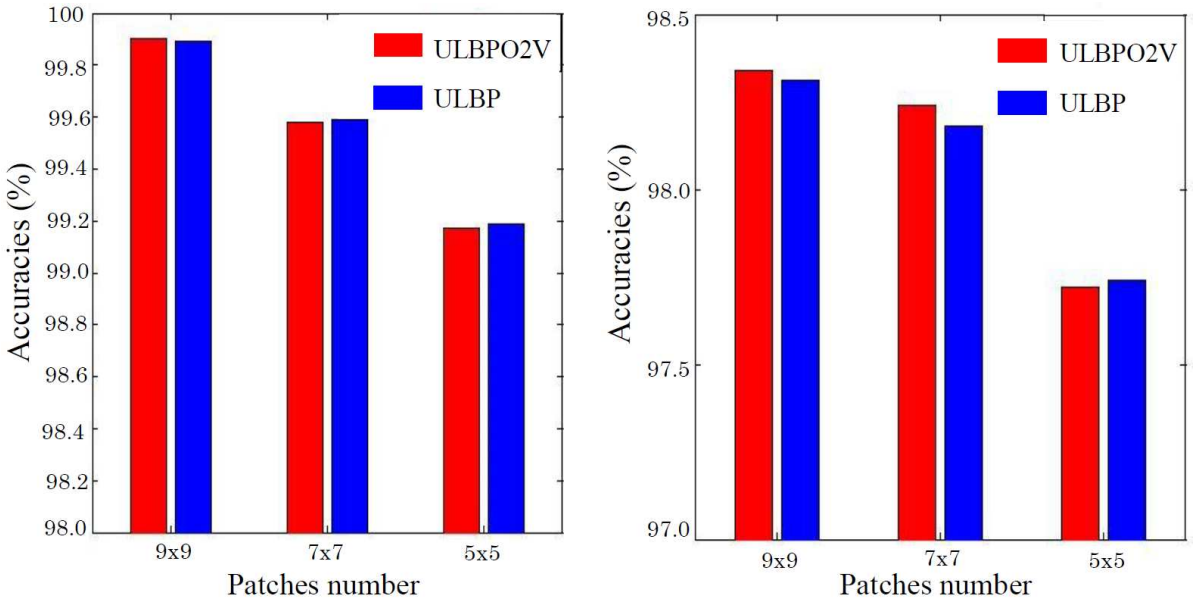

(a) In the Extended Yale B dataset (b) In the CMUPIE dataset

FIGURE 11. Comparing the ULBPO2V and the ULBP

that when the patches number is fixed to 9×9, ULBPO2V not only improves the accuracy but also decreases data dimensions.

4.5. **Investigating the effect of the number of decomposed directions.** The number of decomposed directions of shearlets also has an impact on the accuracy, but very few papers studied its effect. In this paper, we explore the influence of the number of decomposed directions in each level in the AR database. z-axis, y-axis, and x-axis, respectively, represent the number of directions in the 1^{st}, 2^{nd}, 3^{rd} levels. We use colors to express the recognition rates. Figure 12 reports the results. We find that $z = 10$, Shearlets_EF performs relatively well under the condition of illumination and occlusion while $x = 10$, Shearlets_EF works relatively well under the condition of expression. When (z, y, x) is fixed to $(10, 6, 6)$, $(4, 6, 10)$, $(6, 10, 6)$, $(10, 6, 4)$ in the conditions of illumination, expression, 20% occlusion and 40% occlusion respectively, Shearlets_EF achieves the best result.

5. **Conclusions.** In this paper, for the significant edges, we propose an algorithm of face recognition using shearlets edges fusion. Shearlets_EF harvests the advantages of the shearlet transform which can extract anisotropic and directional information effectively, the fusion by the maximum modulus principle which can hold significant edges and structure attribute of the face image, and the ULBPO2V which can reduce dimensions of the histogram and surpass the original ULBP when patches number is fixed to 9×9. The experiments demonstrate that Shearlets_EF is robust to variations and achieves satisfactory result relatively. As a matter of fact, our algorithm does not compare with deep learning method. Deep learning may outstrip Shearlets_EF, but it needs tremendous dataset. In the future work, we will try to conquer the sensitiveness of Shearlets_EF to the patches number and the time consumption problem.

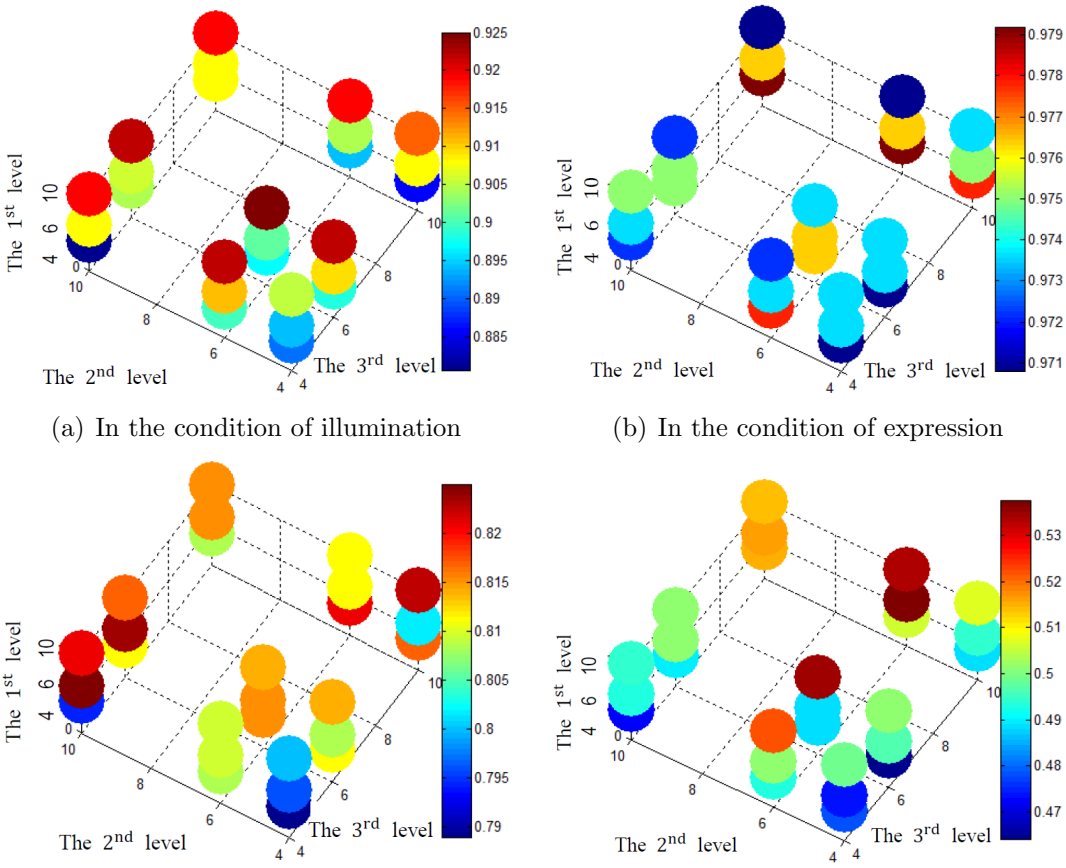

(a) In the condition of illumination

(b) In the condition of expression

(c) In the condition of 20% occlusion

(d) In the condition of 40% occlusion

FIGURE 12. (color online) The influence of the number of directions in each level

REFERENCES

[1] Y. Lu, N. Zeng, Y. Liu et al., A hybrid wavelet neural network and switching particle swarm optimization algorithm for face direction recognition, *Neurocomputing*, vol.155, pp.219-224, 2015.

[2] S. Farokhi, S. M. Shamsuddin, U. U. Sheikh et al., Near infrared face recognition by combining Zernike moments and undecimated discrete wavelet transform, *Digital Signal Processing*, vol.31, pp.13-27, 2014.

[3] C. G. Bertinetto and T. Vuorinen, Automatic baseline recognition for the correction of large sets of spectra using continuous wavelet transform and iterative fitting, *Applied Spectroscopy*, vol.68, no.2, pp.155-164, 2014.

[4] J. Yang, M. Luo and Y. Jiao, Face recognition based on image latent semantic analysis model and SVM, *International Journal of Signal Processing, Image Processing and Pattern Recognition*, vol.6, no.3, 2013.

[5] L. B. Zhang, F. Peng, L. Qin et al., Face spoofing detection based on color texture Markov feature and support vector machine recursive feature elimination, *Journal of Visual Communication and Image Representation*, vol.51, pp.56-69, 2018.

[6] F. A. Pujol, A. Jimeno-Morenilla and J.-L. Sanchez-Romero, Face recognition using a hybrid SVM-LBP approach and the Indian movie face database, *Current Science*, vol.113, no.5, pp.974-977, 2017.

[7] X. Yin and X. Liu, Multi-task convolutional neural network for pose-invariant face recognition, *IEEE Trans. Image Processing*, vol.27, no.2, pp.964-975, 2018.

[8] Y. H. Kim, H. Kim, S. W. Kim et al., Illumination normalisation using convolutional neural network with application to face recognition, *Electronics Letters*, vol.53, no.6, pp.399-401, 2017.

[9] A. Alotaibi and A. Mahmood, Deep face liveness detection based on nonlinear diffusion using convolution neural network, *Signal, Image and Video Processing*, vol.11, no.4, pp.713-720, 2017.

[10] W. P. Choi, S. H. Tse, K. W. Wong et al., Simplified Gabor wavelets for human face recognition, *Pattern Recognition*, vol.41, no.3, pp.1186-1199, 2008.

[11] X. Xie and K. M. Lam, Gabor-based kernel PCA with doubly nonlinear mapping for face recognition with a single face image, *IEEE Trans. Image Processing*, vol.15, no.9, pp.2481-2492, 2006.
[12] A. Brunton, T. Bolkart and S. Wuhrer, Multilinear wavelets: A statistical shape space for human faces, *European Conference on Computer Vision*, pp.297-312, 2014.
[13] K. Guo, G. Kutyniok and D. Labate, Sparse multidimensional representations using anisotropic dilation and shear operators, *International Conference on the Interaction between Wavelets and Splines*, Athens, GA, 2005.
[14] G. Easley, D. Labate and W. Lim, Sparse directional image representations using the discrete shearlet transform, *Applied & Computational Harmonic Analysis*, vol.25, no.1, pp.25-46, 2008.
[15] M. A. Borgi, D. Labate, M. El'Arbi et al., Shearlet network-based sparse coding augmented by facial texture features for face recognition, *International Conference on Image Analysis and Processing*, Springer, Berlin, Heidelberg, pp.611-620, 2013.
[16] B. M. Sujatha, B. V. Venukumar, C. T. Madiwalar et al., Translation based face recognition using fusion of LL and SV coefficients, *Procedia Computer Science*, vol.89, pp.877-886, 2016.
[17] Y. Lu, S. Wang, W. Zhao et al., A novel approach of facial expression recognition based on shearlet transform, *IEEE Global Conference on Signal and Information Processing (GlobalSIP)*, pp.398-402, 2017.
[18] L. M. Po, Y. Li, F. Yuan et al., Face liveness detection using shearlet-based feature descriptors, *Journal of Electronic Imaging*, vol.25, no.4, 2016.
[19] Y. Huang, Y. Zhang and L. Pan, Face recognition algorithm based on differences shearlet characteristic of fast sparse description, *Opto-Electronic Engineering*, 2016.
[20] W. R. Schwartz, R. D. Da Silva, L. S. Davis et al., A novel feature descriptor based on the shearlet transform, *The 18th IEEE International Conference on Image Processing (ICIP)*, pp.1033-1036, 2011.
[21] H. Zhang, X. Wang and Z. Sun, Face recognition based on shearlet multi-orientation adaptive weighted fusion and sparse representation, *Opto-Electronic Engineering*, vol.41, no.12, pp.66-71, 2014.
[22] P. Xie and X. Wang, Face recognition algorithm of collaborative representation based on shearlet transform and uniform local binary pattern, *Journal of Computer Applications*, vol.35, no.7, pp.2056-2061, 2015.
[23] X. Wang, L. Qin, Z. Sun et al., The face recognition based on local shearlet phase quantization, *Opto-Electronic Engineering*, vol.4, 2013.
[24] G. Kutyniok and D. Labate, Resolution of the wavefront set using continuous shearlets, *Transactions of the American Mathematical Society*, vol.361, no.5, pp.2719-2754, 2009.
[25] T. Ojala, M. Pietikäinen and D. Harwood, A comparative study of texture measures with classification based on featured distributions, *Pattern Recognition*, vol.29, no.1, pp.51-59, 1996.
[26] L. Zhang, M. Yang and X. Feng, Sparse representation or collaborative representation: Which helps face recognition?, *IEEE International Conference on Computer Vision (ICCV)*, pp.471-478, 2011.
[27] A. M. Martinez, The AR face database, *CVC Technical Report24*, 1998.
[28] R. Gross, I. Matthews, J. Cohn et al., Multi-PIE, *Image and Vision Computing*, vol.28, no.5, pp.807-813, 2010.
[29] A. S. Georghiades, P. N. Belhumeur and D. J. Kriegman, From few to many: Illumination cone models for face recognition under variable lighting and pose, *IEEE Trans. Pattern Analysis and Machine Intelligence*, vol.23, no.6, pp.643-660, 2001.
[30] G. B. Huang, M. Mattar, T. Berg et al., Labeled faces in the wild: A database for studying face recognition in unconstrained environments, *Workshop on Faces in 'Real-Life' Images: Detection, Alignment, and Recognition*, 2008.
[31] J. Wen, X. Fang, J. Cui et al., Robust sparse linear discriminant analysis, *IEEE Trans. Circuits and Systems for Video Technology*, 2018.
[32] Y. Xu, Z. Li, B. Zhang et al., Sample diversity, representation effectiveness and robust dictionary learning for face recognition, *Information Sciences*, vol.375, pp.171-182, 2017.
[33] P. Zhu, L. Zhang, Q. Hu et al., Multi-scale patch based collaborative representation for face recognition with margin distribution optimization, *European Conference on Computer Vision*, pp.822-835, 2012.